

UNIVERSITÄT LEIPZIG

INTERNATIONAL PHYSICS STUDIES PROGRAM

LABORATORY REPORT

Rotation-Vibration Spectra of Molecules

Author:

Ena OSMIC
Luka GLOMAZIC

Supervisor:

Dr. Richard REZNICEK

May 29, 2019



UNIVERSITÄT LEIPZIG
FAKULTÄT FÜR PHYSIK
UND GEOWISSENSCHAFTEN

Contents

1	Introduction	2
2	Theory	3
2.1	Infrared Spectroscopy	3
2.2	Dumbbell Model of Diatomic Molecule	3
2.3	Rotation Vibration Spectra	6
2.4	Intensity of Absorption Lines	8
2.5	Interference Method	9
3	Experimental Setup	9
4	Experimental Tasks	11
5	Results ans Discussion	11
5.1	Task 1	11
5.2	Task 2	13
5.3	Task 3	16
5.4	Task 4	18
5.5	Task 5	20
5.6	Task 6	23
6	References	24

1 Introduction

Rotational–vibrational spectroscopy is a branch of molecular spectroscopy concerned with infrared and Raman spectra of molecules in the gas phase.

High-resolution infrared (IR) spectroscopy is the key to the quantum-state-resolved analysis of molecular rotation–vibration spectra and the consequent understanding of the quantum dynamics of molecules. In the IR range of the spectrum, however, which is important for the study of combined rotational–vibrational excitation, experimental resolution was sufficient in the past only for the simpler diatomic and polyatomic molecules, largely limited by the technology of grating or more generally dispersive spectrometers. There has been substantial development of IR and Raman spectroscopy at much higher resolution in recent decades, based on laser technology, on one hand, and interferometric Fourier transform infrared (FTIR) spectroscopy, on the other hand. This has made the rotation–vibration spectra of much more complex molecules accessible to the full analysis of the rotational–vibrational fine structure and the frontier in this area of research is moving toward even larger polyatomic molecules.

During this experiment, we were investigating the rotational-vibrational spectra of the diatomic molecule of hydrochloric acid (*HCl*).

2 Theory

2.1 Infrared Spectroscopy

Infrared spectroscopy involves the interaction of infrared radiation with matter. It covers a range of techniques, mostly based on absorption spectroscopy. As with all spectroscopic techniques, it can be used to identify and study chemicals.

Infrared spectroscopy exploits the fact that molecules absorb frequencies that are characteristic of their structure. These absorptions occur at resonant frequencies, i.e. the frequency of the absorbed radiation matches the vibrational frequency. The energies are affected by the shape of the molecular potential energy surfaces, the masses of the atoms, and the associated vibronic coupling. The infrared portion of the electromagnetic spectrum is usually divided into three regions; the near-, mid- and far- infrared, named for their relation to the visible spectrum.

Even though it can be used to study samples of all states of matter, it is mostly used for determining properties and concentration of molecules in gases. This is usually achieved with the help of transmission spectra.

Beer–Lambert law

The Beer-Lambert law relates the attenuation of light to the properties of the material through which the light is traveling.

For each wavelength of light passing through the spectrometer, the intensity of the light passing through the reference cell is measured. This is usually referred to as I_0 . The intensity of the light passing through the sample cell is also measured for that wavelength - given the symbol, I . The relationship between those is given by:

$$I(\lambda) = I_0(\lambda)e^{\alpha(\lambda)cd} \quad (1)$$

where d is the thickness of the material and c is the concentration the material has been diluted with.

Spectrometer used in this experiment, *Spectrum 100*, allows to access the mid infrared range. Various physical quantities are typically used in infrared spectroscopy to characterize the spectral position: the vacuum wavelength λ , the wavenumber $\bar{\nu}$, the frequency ν and the angular frequency ω :

$$\bar{\nu} = \frac{1}{\lambda} = \frac{\nu}{c} = \frac{\omega}{2\pi c} \quad (2)$$

2.2 Dumbbell Model of Diatomic Molecule

In the dumbbell model, the two atoms are considered to be point masses which are connected by binding forces yielding a certain distance between them. The dumbbell can rotate and vibrate with frequencies which depend on the atomic masses, the binding forces and the interaction between rotational and vibrational motion.

The rotation of a diatomic molecule can be described by the **rigid rotor model**. The dumbbell has two masses set at a fixed distance from one another and spins around its center of mass (COM). This model can be further simplified using the concept of reduced mass which allows the problem to be treated as a single body system.

The simplest form of this model is the **rigid rotator with spatially fixed rotational axis**.

Using the *center of mass theorem*, one can find the distance between the atoms inside the molecule and the moment of inertia of the system.

$$I = \mu r^2 \quad (3)$$

where $\mu = \frac{m_1 m_2}{m_1 + m_2}$ and $r = r_1 + r_2$

The energy eigenvalues can be calculated using quantum mechanics. The Schrödinger equation $\Delta\Psi + \frac{8\pi^2 m}{\hbar^2}(E - U)\Psi = 0$ needs to be solved for the case of rotating dumbbell.

Solving, we find that the energy can only take discrete values:

$$E_m = m^2 \frac{\hbar^2}{8\pi^2 \mu r^2} \quad (4)$$

with $m = 0, \pm 1, \pm 2\dots$

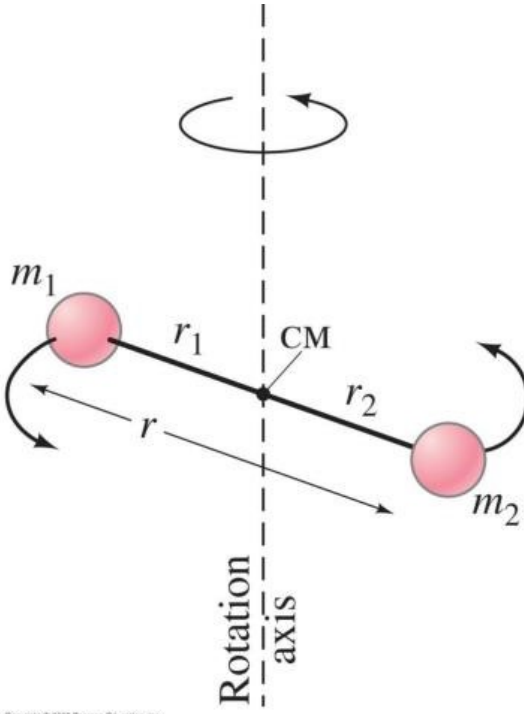


Figure 1: A diatomic molecule can rotate around the vertical axis. The rotational energy is quantized.

In reality, the rotational axis of a diatomic molecule is not spatially fixed which leads us to a slightly more complex model of a **rigid rotator with spatially variable rotational axis**. This means that wave function dependence on angular coordinate now needs to be taken into account.

We will write out the Schrödinger equation in spherical coordinates:

$$\frac{1}{r} \left\{ \frac{1}{\sin\theta} \frac{\partial}{\partial\theta} \left(\sin\theta \frac{\partial\psi}{\partial\theta} \right) + \frac{1}{\sin^2\theta} \frac{\partial^2\psi}{\partial\Phi^2} \right\} + \frac{8\pi^2\mu E}{h^2} \psi = 0 \quad (5)$$

Yet again, the solution leads to discrete energy values.

$$E(J) = \frac{\hbar^2}{8\pi^2\mu r^2} J(J+1) \quad (6)$$

With J being the rotational number ($J = 0, 1, 2\dots$).

We define the rotational constant B :

$$B = \frac{\hbar}{8\pi^2 c l} \quad (7)$$

and the rotational term F :

$$F(J) = \frac{E(J)}{hc} = BJ(J+1) \quad (8)$$

Since the rotational term has the dimension of a wavenumber it is well suitable for analysis of spectra plotted against the wavenumber. The selection rule $\Delta J = \pm 1$ holds for the transitions between rotational states.

The energy difference for a transition between two vibrational states is defined as:

$$E(J+1) - E(J) = 2hcB(J+1) \quad (9)$$

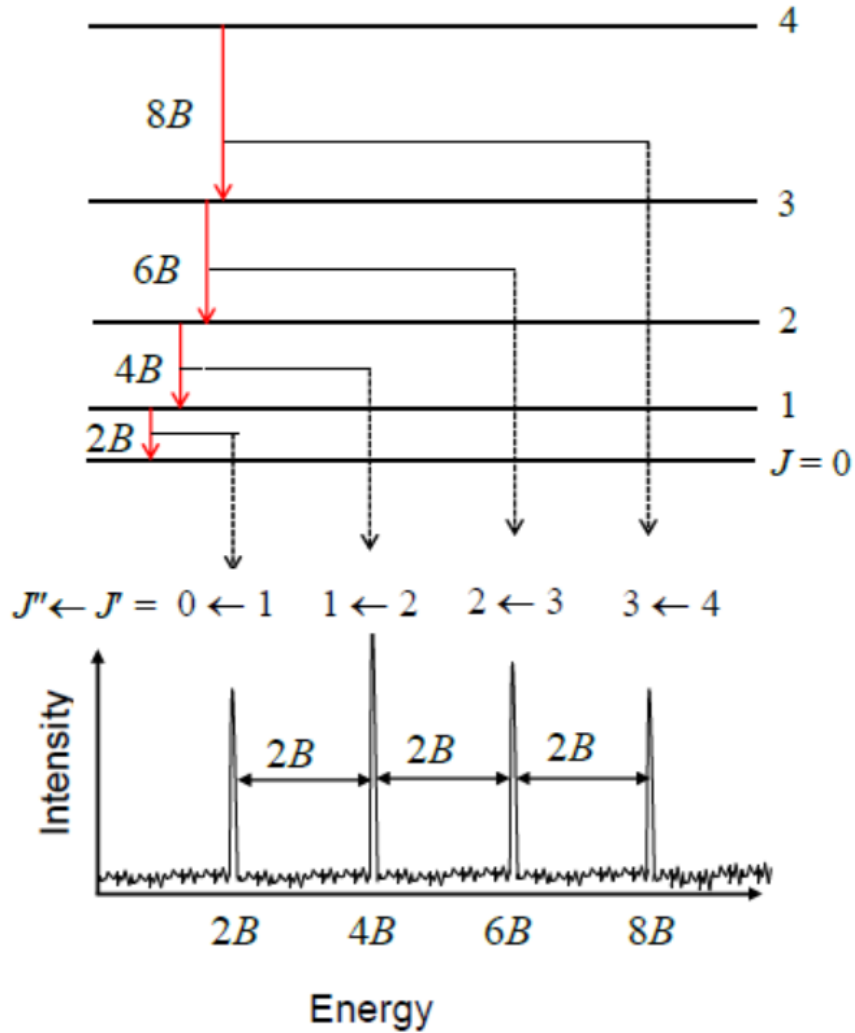


Figure 2: Energy levels and line positions calculated in the rigid rotor approximation.

The image above shows that the rotational spectrum consists of equidistant absorption lines, with distance between them being $\nu = 2B$.

After we have explained the rotation of the molecule, we also have to take into account that molecules vibrate against each other and that motion can be described with the use of the **harmonic oscillator approximation**.

If we let x_1 and x_2 be the displacements of the atoms from the equilibrium, and if $x = x_1 - x_2$, the equation of motion becomes

$$\ddot{x} = -\frac{k}{\mu}x \quad (10)$$

which is simply the equation of motion of a harmonic oscillator with a resonance wavenumber:

$$\bar{\nu}_s = \frac{1}{2\pi c} \sqrt{\frac{k}{\mu}} \quad (11)$$

In the quantum mechanical treatment, the Schrödinger equation must be solved. For this, the potential energy is required:

$$U = 2\pi^2 c^2 \bar{\nu}_s^2 \mu x^2 \quad (12)$$

The Schrödinger equation for the x components then reads:

$$\frac{d^2\psi}{dx^2} + \frac{8\pi^2\mu}{h^2}(E - 2\pi^2c^2\bar{\nu}_s\mu x^2)\psi = 0 \quad (13)$$

Resulting eigenvalues are

$$E(n) = hc\bar{\nu}_s\left(n + \frac{1}{2}\right) \quad (14)$$

with vibrational quantum number $n = 0, 1, 2, \dots$

As for the rotator, only discrete energy eigenvalues are allowed and thus, according to quantum mechanics, only dipole transitions with $\Delta n = \pm 1$, are allowed. The respective transition energies are

$$E(n+1) - E(n) = hc\bar{\nu}_s \quad (15)$$

The vibrational term can now be obtained

$$G(n) = \frac{E(n)}{hc} = \bar{\nu}_s\left(n + \frac{1}{2}\right) \quad (16)$$

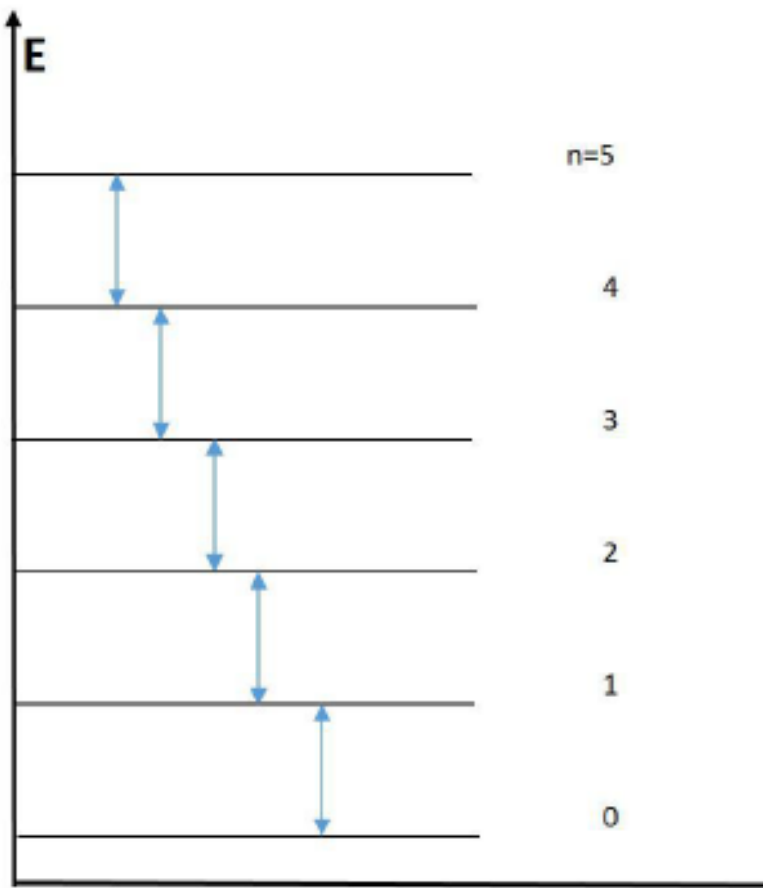


Figure 3: Energy scheme of harmonic oscillator.

2.3 Rotation Vibration Spectra

Previously, the rotation and vibration have been treated autonomously, but in real physical system they coincide and occur simultaneously. Now, we will be looking at their combined effect, starting with **molecules with rigid axis**.

Combining equations 9 and 14 we find the total energy of the rotating oscillator:

$$E(n, J) = hcBJ(J+1) + hc\bar{\nu}_s\left(n + \frac{1}{2}\right) \quad (17)$$

Equivalently as before, we define a rotational-vibrational part $T(n, J)$

$$\frac{E(n, J)}{hc} = T(n, J) = BJ(J+1) + \bar{\nu}_s\left(n + \frac{1}{2}\right) \quad (18)$$

With the selection rules being $\Delta J = \pm 1$ and $\Delta n = 0, \pm 1$ we have three possible cases:

- transitions corresponding to $\Delta J = \pm 1$ and $\Delta n = 0$ result purely in rotational spectrum
- for transitions corresponding to $\Delta J = 1$ and $\Delta n = 1$, the difference between rotational-vibrational terms corresponds to wavenumber of certain transitions

$$T(n+1, J+1) - T(n, J) = \bar{\nu}_s + 2B(J+1) = \bar{\nu}_R(J) \quad (19)$$

These transitions are called *R-branch*.

- for transitions corresponding to $\Delta J = -1$ and $\Delta n = 1$,

$$T(n+1, J-1) - T(n, J) = \bar{\nu}_s - 2B(J+1) = \bar{\nu}_P(J) \quad (20)$$

These absorption lines are so-called *P-branch*.

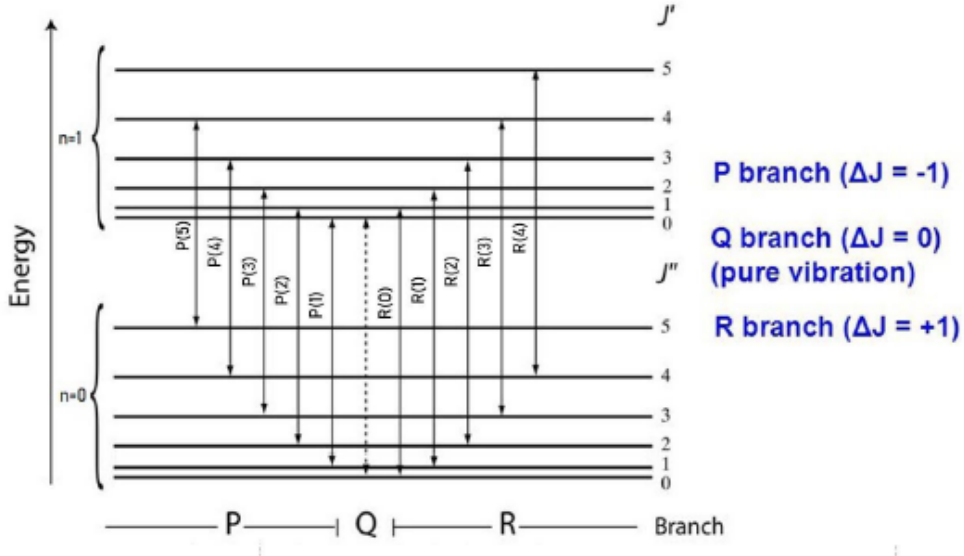


Figure 4: Energy scheme of a harmonic oscillator.

Wavenumber of the vibrational transition as well as the rotational constant can be obtained from the following relations:

$$\bar{\nu}_R(0) + \bar{\nu}_P(1) = 2\bar{\nu}_s \quad \text{and} \quad \bar{\nu}_R(0) - \bar{\nu}_P(1) = 4B \quad (21)$$

Spectrometer used in this experiment allows for very precise measurements which means that effects due to **non-rigid axis of the molecule** can be studied. In reality, centrifugal force of the rotation enlarges the distance between the atoms which results in changes to moment of inertia, rotational constant and etc. Hence, we introduce centrifugal distortion constant D . Another distinction is that due to anharmonicity effects

moment of inertia and constants B and D become dependent on the vibrational quantum number. Taking this effect into consideration, rotational term is rewritten as:

$$F_n(J) = B_n J(J+1) - D_n J^2(J+1)^2 \quad (22)$$

Likewise as before, transitions from $n = 0$ to $n = 1$ of the R-branch are characterized by following equation:

$$\bar{\nu}_R = \bar{\nu}_s + (2B_1 - 4D_1) + J(3B_1 - B_0 - 12D_1) + J^2(B_1 - B_0 - 13D_1 - D_0) - J^3(6D_1 - 2D_0) - J^4(D_1 - D_0) \quad (23)$$

And equation for P-branch is as follows:

$$\bar{\nu}_P = \bar{\nu}_s - J(B_1 + B_0) + J^2(B_1 - B_0 - D_1 + D_0) + 2J^3(D_1 + D_0) - J^4(D_1 - D_0) \quad (24)$$

We are able to condense these 2 equations into a single one with use of *running index* i and further simplify it due to $D_n \ll B_n$ and $D_n \approx D_{n+1}$

$$\bar{\nu}_i = \bar{\nu}_s + (B_1 - B_0)i + (B_1 - B_0)i^2 - 2(D_1 + D_0)i^3 \quad (25)$$

Running index i is assigned to quantum number J according to the table below

	P-branch	R-branch
J	3 2 1	0 1 2
i	-3 -2 -1	1 2 3

2.4 Intensity of Absorption Lines

The spectral position of the absorption lines allow to determine the physical parameters of a diatomic molecule.

The intensity distribution in a spectral line is determined by the optical properties of the absorbing or emitting atoms, but depends also on the external conditions to which these atoms are subjected.

Absorption maxima found in rotation-vibration spectrum belonging to R- and P-branch respectively can be used to determine rotational constant and the wave number of the vibrational transition. For that, absorption coefficient in dependence of the wavenumber is required.

For a transition between lower (i) and upper (j) state, absorption coefficient is

$$\alpha^{ji} = W_{ij} N_i h c \bar{\nu}_{ji} \quad (26)$$

where W_{ij} is the Einstein coefficient for absorption of light with wavenumber $\bar{\nu}_{ji}$ and N_i is the number of molecules in the lower state i per unit volume.

Due to the fact that during the experiment, the system is in thermodynamic equilibrium, the number of molecules with particular energy E is given by *Maxwell Boltzmann distribution*.

$$N(E) = \frac{\eta}{Q_r} e^{-\frac{E}{k_B T}} \quad (27)$$

where η is the total number of molecules, Q_r is the partition function, k_B is the Boltzmann constant and T is the temperature.

Equation above can be inserted into equation (gore ce pisati neka tako da ubaci ovdje broj) to obtain:

$$N(J, n=0) = \frac{\eta}{Q_r} (2J+1) e^{-\frac{hcB(J+1)}{k_B T}} e^{-\frac{hc\bar{\nu}_s(n+1/2)}{k_B T}} \quad (28)$$

Absorption coefficient then becomes

$$\alpha = C \bar{\nu} (2J+1) e^{-\frac{hcB(J+1)}{k_B T}} \quad (29)$$

where the constant C is defined as

$$C = \frac{hcW\eta}{Q_r} e^{-\frac{hc\bar{\nu}_s(n+1/2)}{k_B T}} \quad (30)$$

2.5 Interference Method

If a light beam is guided through an empty cuvette, the light is reflected, which results in interference. These interferences depend on the wavelength of the light, the thickness and index of refraction in the cavity, the angle of incidence. In the spectrum, they appear as a periodic modulation of the intensity.

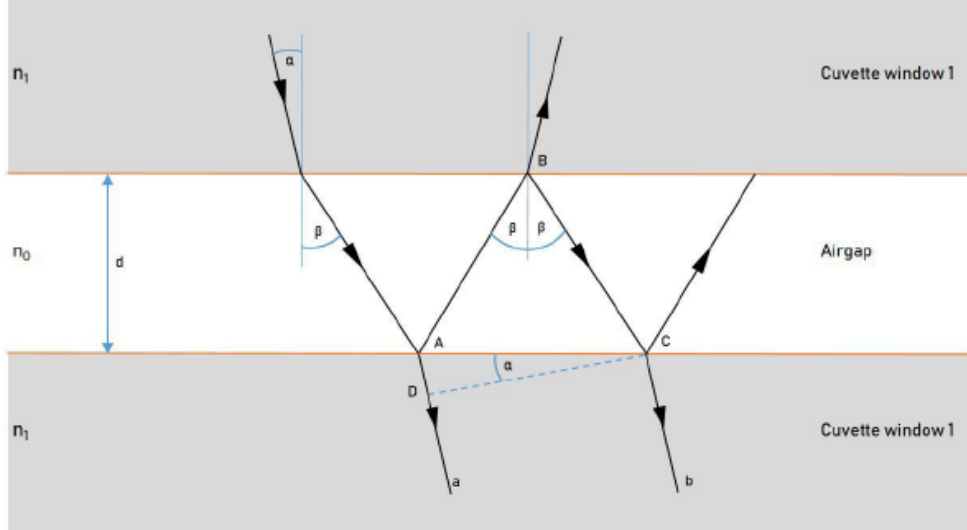


Figure 5: Beam path through a cuvette.

Optical path difference Δ can be derived from the geometrical optics and Snell's law by:

$$\Delta = 2n_0 d \cos \beta \quad (31)$$

Maximum and minimum in transmission are observed for wavenumbers that follow the following relations respectively

$$2n_0 d = \frac{N}{\nu} \quad (32)$$

with the order of extrema $N = 0, 1, 2, \dots$

Including the equation below, these relations can be used for determining the gap thickness.

$$2n_0 d = (N + 1/2) \frac{1}{\nu} \quad (33)$$

Yielding in the end, for a maximum of order N_1 at $\bar{\nu}_1$ and a maximum of order N_2 at $\bar{\nu}_2$, the gap thickness in question:

$$d = \frac{N_1 - N_2}{2n_0(\bar{\nu}_1 - \bar{\nu}_2)} \quad (34)$$

3 Experimental Setup

For the purposes of this experiment, the *FTIR spectrometer PerkinElmer Spectrum 100* was used.

This specific spectrometer is based on a modified Michelson interferometer, which is primarily due to the compact design of device. Instead of a translating mirror, a mirror pair is used together with a fixed mirror. By the rotation of the mirror pair around a common axis, the beam path between the beam splitter and the fixed mirror is changed. The path difference is determined based on the interferences of a HeNe laser, which is also coupled into the spectrometer.

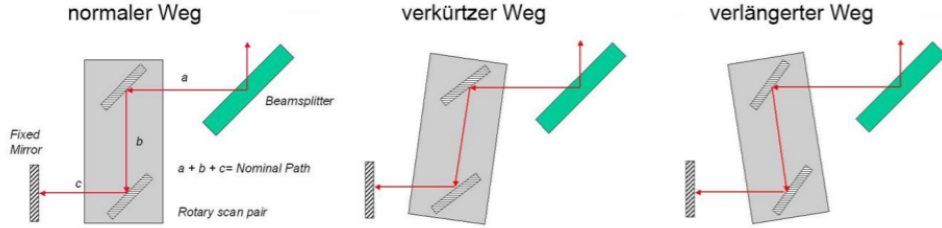


Figure 6: Beam path.

A so-called “glowbar” (alternatively called “Norton source”) is used as light source. This is a U-shaped bar made from doped SiC, which is heated by a current flow. It approximately emits a black body spectrum with a maximum in the mid infrared.

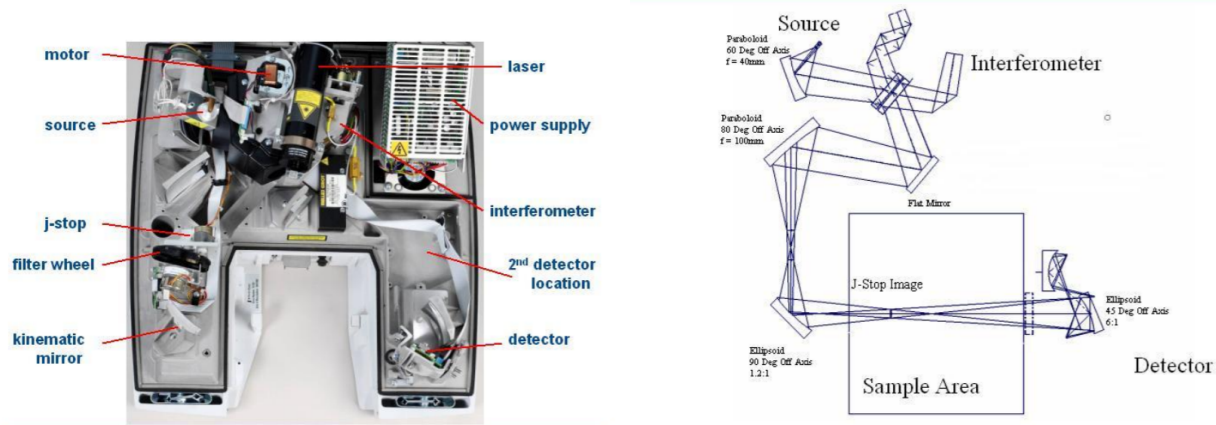


Figure 7: Images of *Spectrum 100* interior and optics, respectively.

4 Experimental Tasks

Task 1

Verify the calibration of the wavenumber scale of the infrared spectrometer Spectrum 100 using water vapor and polystyrene calibration bands. Plot the experimentally determined deviations and discuss them

Task 2

Acquire interferograms of the water vapor spectrum using different mirror ranges of the interferometer. Obtain the spectra by applying a Fourier transformation to these interferograms. Calibrate the wavenumber scale of the thereby obtained spectra using the values for the water vapor bands. Determine step size of the optical path from the band width of the spectrum. Discuss the influence of the interferogram length and the applied zero-filling and apodisation on the spectral resolution based on the spectra. Based on the calculated step size, give the theoretical spectral resolution in dependence on the recorded data point count.

Task 3

Determine the detected signal strength in the blocking range of a glass and a $NaCl$ blocking filter.

Task 4

Determine the gap width of a cuvette using the interference method. For that, plot of ΔN over $\bar{\nu}_N$ and determine the gap width and its mean square error using the method of linear regression.

Task 5

Acquire the rotation vibration spectrum of hydrogen chloride (HCl) gas using an adequate spectral resolution and determine the spectral position of the absorption bands. Calculate the wavenumber of the pure vibration transition, the force constant, the rotation constant, the distance of the two atoms in the molecule and the moment of inertia. Further, determine the vibration-dependent rotation constant B_n , the centrifugal distortion constant D as well as the spectral splitting due to the different isotopes. Determine the relation of abundance of the isotopes using the Lambert Beer law.

Task 6

Model the intensities of the absorption minima in the P branch using the theoretical absorption coefficient. Obtain the temperature as a free parameter in the model.

5 Results ans Discussion

5.1 Task 1

Calibration of the spectrometer was performed using water vapor present in the detector chamber of the instrument and polystyrene calibration bands provided by the manufacturer.

Position of certain spectral features was compared to the calibration band table provided in the lab manual.

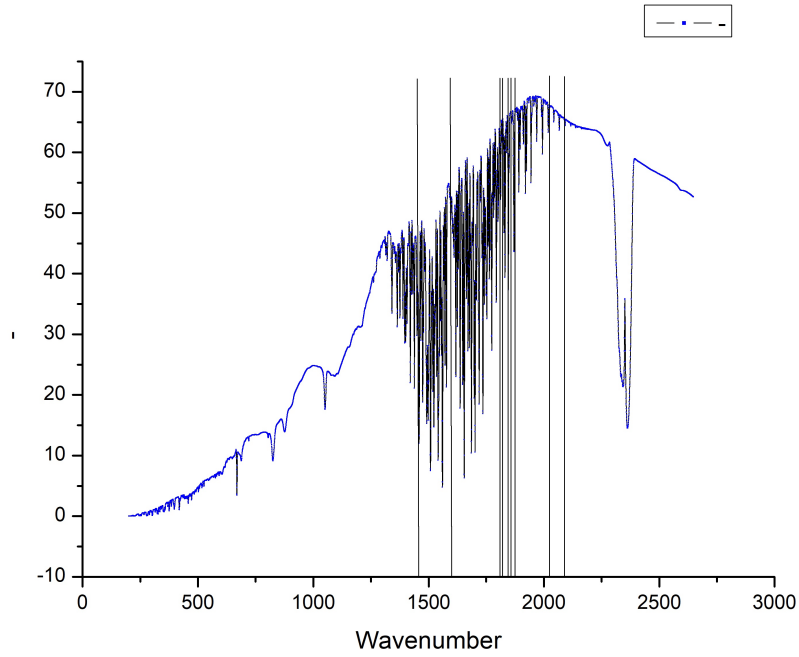


Figure 8: Water vapor calibration bands. The lines on the graph represent the calibration bands provided by the manual.

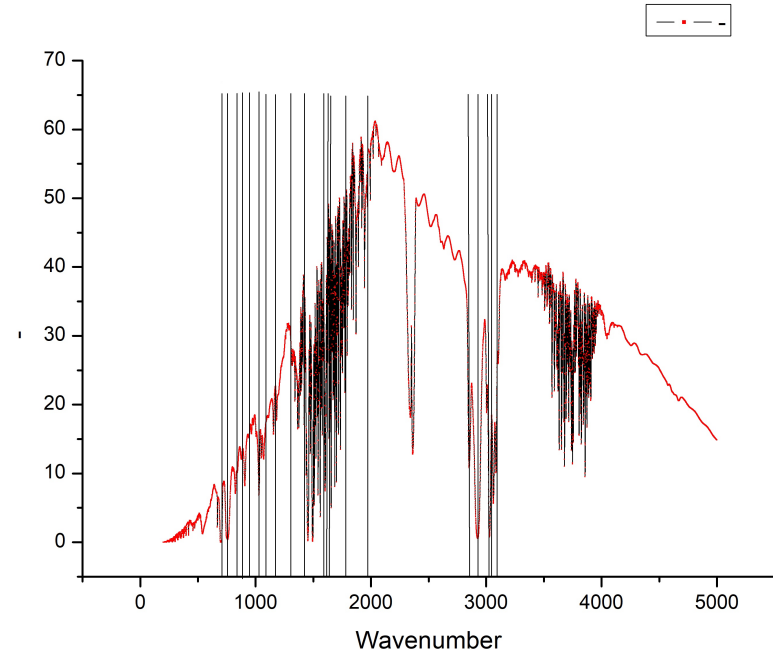


Figure 9: Polystyrene calibration bands. The lines on the graph represent the calibration bands provided by the manual.

Polystyrene proved to more useful tool for calibration, as the signal was less "noisy" and correlation between

calibration bands and measured spectra can be clearly seen. These results are as expected, since water vapor is much more dependent on changes in environmental conditions such as temperature, humidity, etc.

When comparing the spectral positions of predicted and recorded values, no indication of directional systematic error was determined, i.e. both positive and negative deviations from predicted values are found. Average deviation is found to be $\pm 1.46781 \frac{1}{cm}$, and we will consider this as a measurement uncertainty for the rest of the experiment.

5.2 Task 2

Interferograms of water vapor spectrum were recorded using mirror ranges from 8000 to 32000 data points. Then, Fourier transformation was applied in OriginLab with varying zero-filling and apodisation values.

Data was processed according to the following table:

No.	Range	Zero-filling	Apodisation
1	-8000/8000	5	Square
2	-8000/16000	3	Bartlett
3	-8000/32000	None	Blackman

Table 1: Fourier transformation settings.

In order to calibrate the wavenumber scale, we have located the dip in our obtained spectra to be at the frequency position of $f = 0.1489 Hz$, which corresponds to the $\bar{\nu} = 2363.7 \frac{1}{cm}$.

Additionally, to calculate the necessary sampling interval of FFT, we divide

$$\frac{f}{\bar{\nu}} = 0.0000631957671$$

Futhermore, to obtain the step size of the optical path, we will take the wavenumber of the upper end of the spectrum and calculate:

$$\Delta x = \frac{1}{2\bar{\nu}_{max}} = 0.00012639 cm$$

The graphs obtained using the FFT are shown below. Fourier transform is the process of calculating the wave intensity at each period from the sum at all wave periods. Applying Fourier transform to an interferogram obtains the intensity at each period, that is, at each wavelength.

Increase in interferogram length results in increase of recorded data points which in turn decreases the noise of the signal.

Even though zero filling increases the number of data points in the spectrum, spectral resolution is not increased because these additional points do not posses any new information. Increase in zero filling factor results in a "smoother" spectra which can be useful when identifying particular spectral features.

Now we arrive to apodization. It is the process of altering a signal (such as one emitted by an electrical sensor) to make its mathematical description smoother and more easily manipulatable. in our experiment, apodization serves as a tool to minimize any leakage effect which can be a result from the abrupt cut-off of measured interferogram. Apodization will reduce interference-like structures which are caused by leakage effect, but at the same time, the spectral resolution will decrease.

Formula below defones wavenumber difference which is resolvable from the spectrum for a given data point range (n):

$$\Delta\bar{\nu} = \frac{2\bar{\nu}_{max}}{n}$$

Higher resolution corresponds to smaller $\Delta\bar{\nu}$ that can be detected.

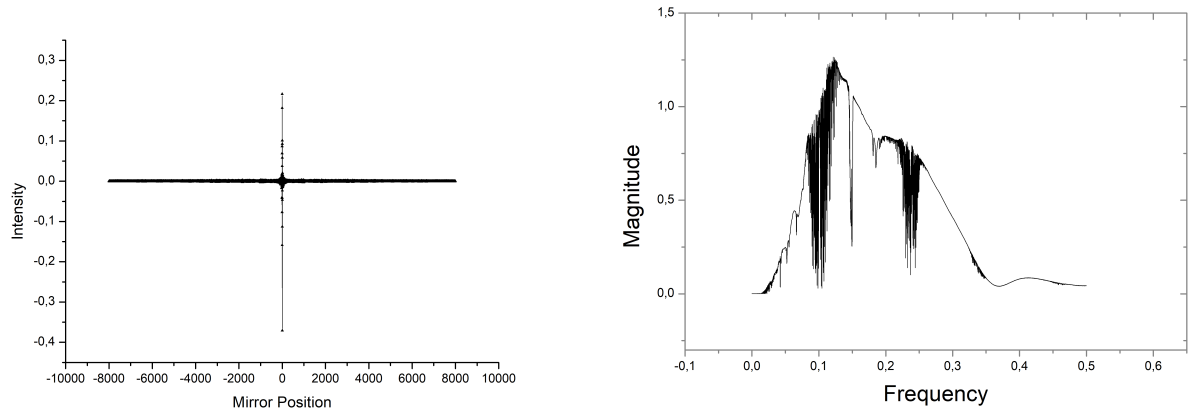


Figure 10: Interferogram and obtained spectra for $(-8000)-(8000)$ range, respectively.

$$\Delta\bar{\nu}_1 = 0.988948 \frac{1}{cm}$$

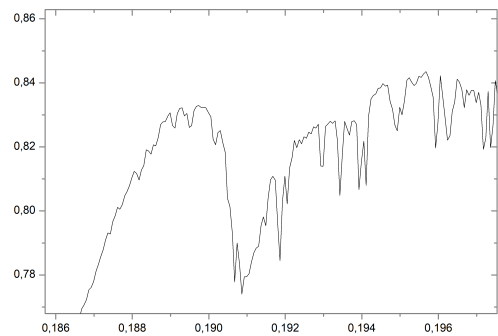


Figure 11: Apodization of the respective spectra, zoomed in.

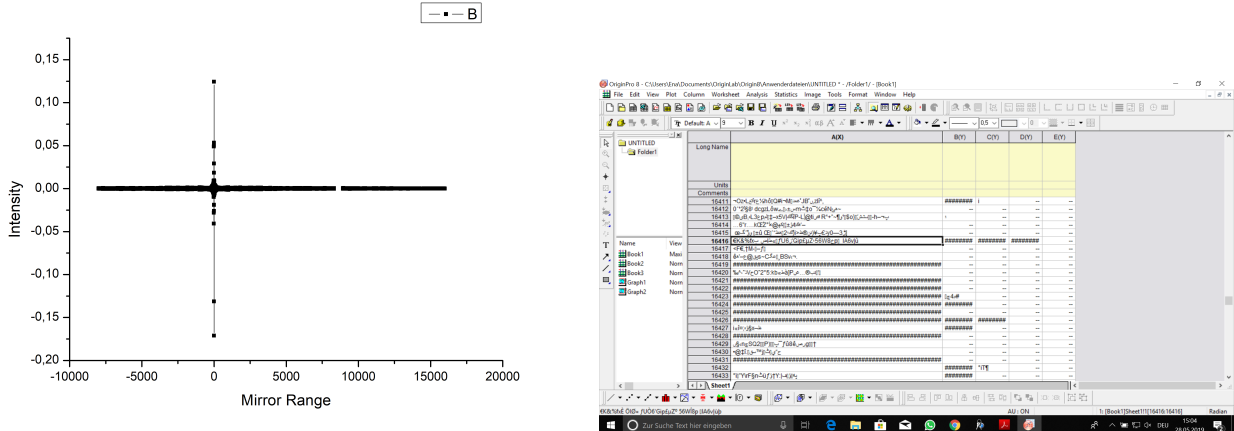


Figure 12: Interferogram for $(-8000)-(16000)$ range. Unfortunately, as seen in the screenshot taken in Origin, some of our data was missing due to unknown reasons. With that being said, it was impossible for us to perform the FFT since the program continued to report a failure.

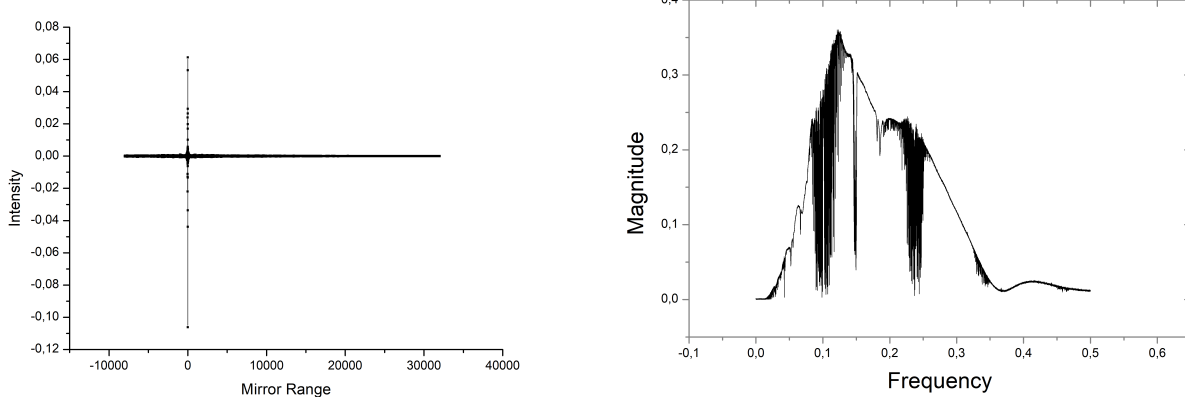


Figure 13: Interferogram and obtained spectra for $(-8000)-(32000)$ range, respectively.

$$\Delta\bar{\nu}_1 = 0.39557 \frac{1}{cm}$$

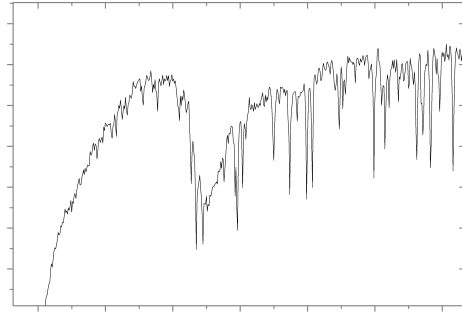


Figure 14: Apodization of the respective spectra, zoomed in.

5.3 Task 3

In this task, the blocking range of glass and $NaCl$ blocking filter has been measured by detecting the signal strength of acquired spectra.

This was done by taking "background" spectra (i.e. spectra of water vapor without blocking filters) and spectra with blocking filters and then overlaying these two on one graph. We determine the following:

In case of a glass blocking filter, the big disparity in measured signal strength almost across all wavenumbers except for the region of higher wavenumbers ($\geq 3600 \frac{1}{cm}$) for which intensity of measured signal is not greatly effected. In the middle region ($2300 - 3500 \frac{1}{cm}$), signal strength is decreased significantly (around 80%). In the lower region ($\leq 2150 \frac{1}{cm}$), signal strength effectively goes to zero.

For the $NaCl$ blocking filter, the situation differs since there are no big disparities like for the case of glass filter. In the region $\geq 2100 \frac{1}{cm}$ we see an almost constant decrease, whereas for the rest of the graph the difference is hardly noticeable.

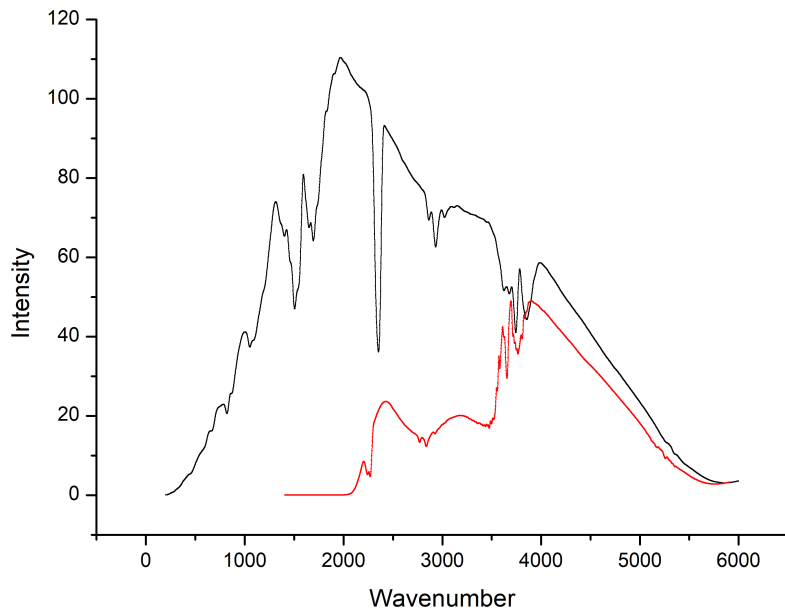


Figure 15: Black graph represents the water vapor background vs the glass blocking filter in red.

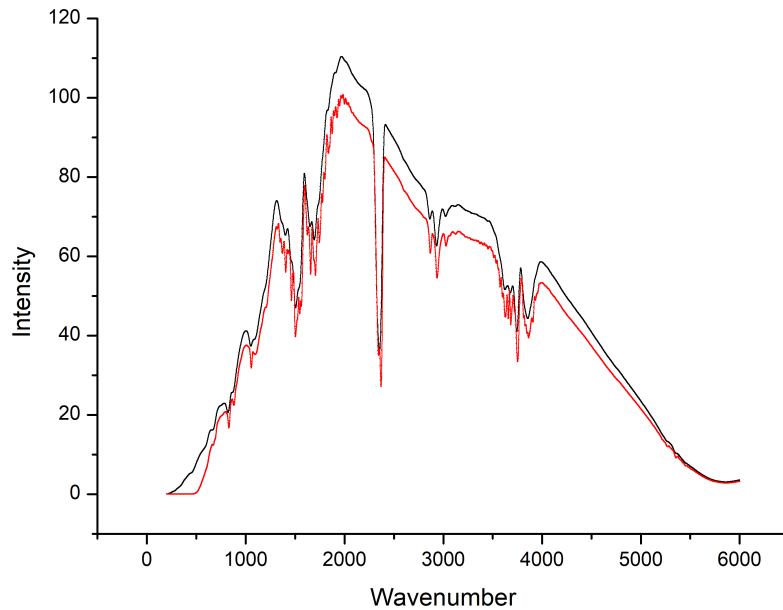


Figure 16: Black graph represents the water vapor background vs the $NaCl$ blocking filter in red.

In order to determine the **stray light** we will divide the spectra of blocking filters with background spectra, effectively blocking a portion of the incoming spectrum and then measuring residual light at given wavenumbers.

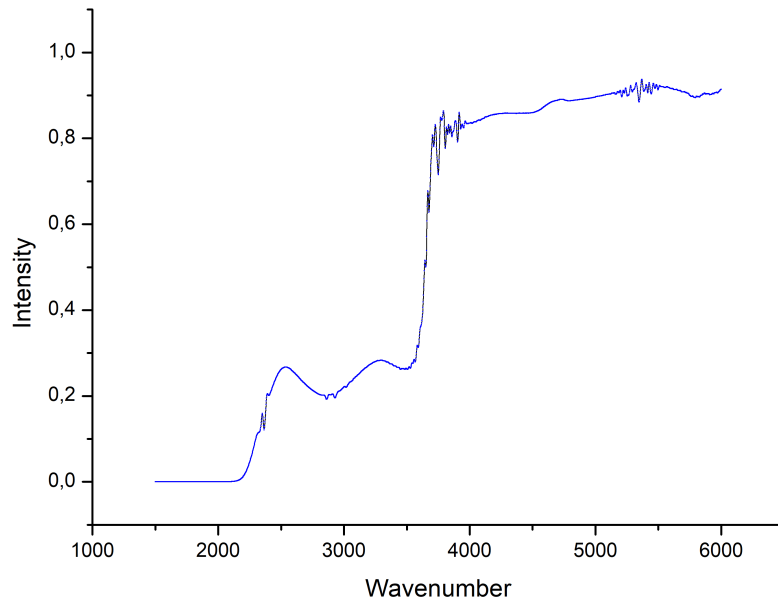


Figure 17: Stray light for glass blocking filter.

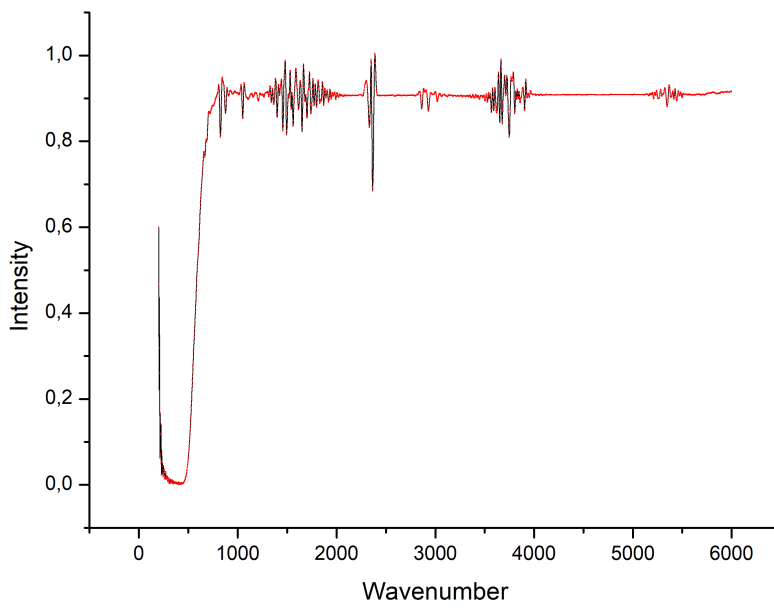


Figure 18: Stray light for $NaCl$ blocking filter.

From the graph, we can see that a signal increases across most of the spectral range with the highest peak being at $3760 \frac{1}{cm}$.

For the $NaCl$ blocking filter, we have an increase in signal strength at $2316 \frac{1}{cm}$, $2920 \frac{1}{cm}$, $3612 \frac{1}{cm}$ and $5290 \frac{1}{cm} \pm 1.46781 \frac{1}{cm}$.

5.4 Task 4

In this task, the gap width of KBr cuvette was determined using the interference method.

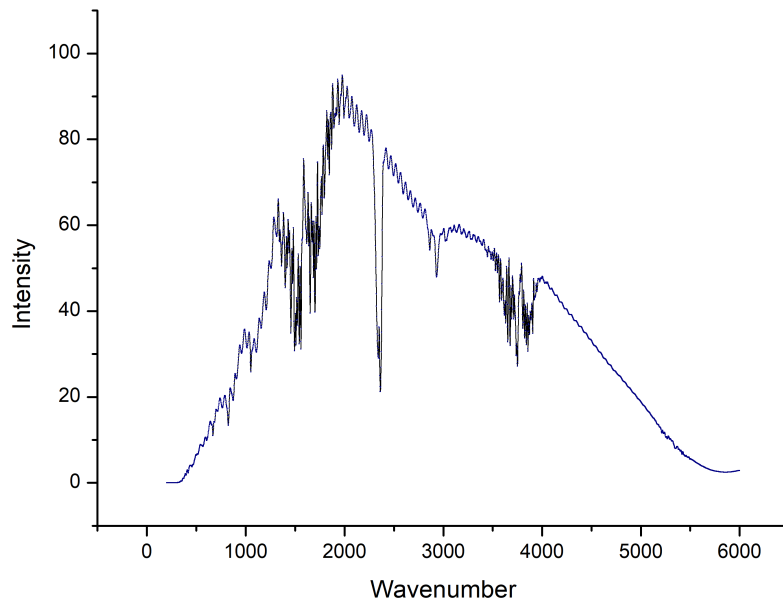


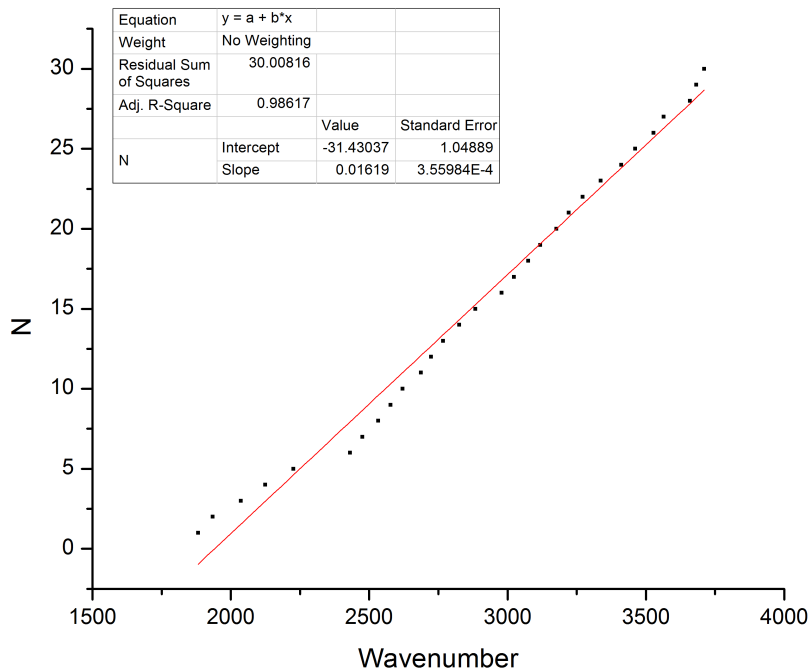
Figure 19: Transmission spectrum of KBr cuvette.

Gap width d was resolved by using the method of **linear regression** and the following formula:

$$\Delta N = 2d\Delta\bar{\nu} \quad (35)$$

From the graph above, 30 points of interference extrema were extracted and plotted against over the corresponding wavelength.

Although we have noticed that the graph has slight offset after the first five values, it levels out in the latter. To average the slope, linear fit was used. The value of the slope is $s = 0.01619 \pm 0.0003559 \text{ cm}$.



Due to the fact that the slope corresponds to $2d$, $d = 0.008095 \pm 0,0001853 \text{ cm}$.

5.5 Task 5

For this task the rotation vibration spectra of HCl was obtained.

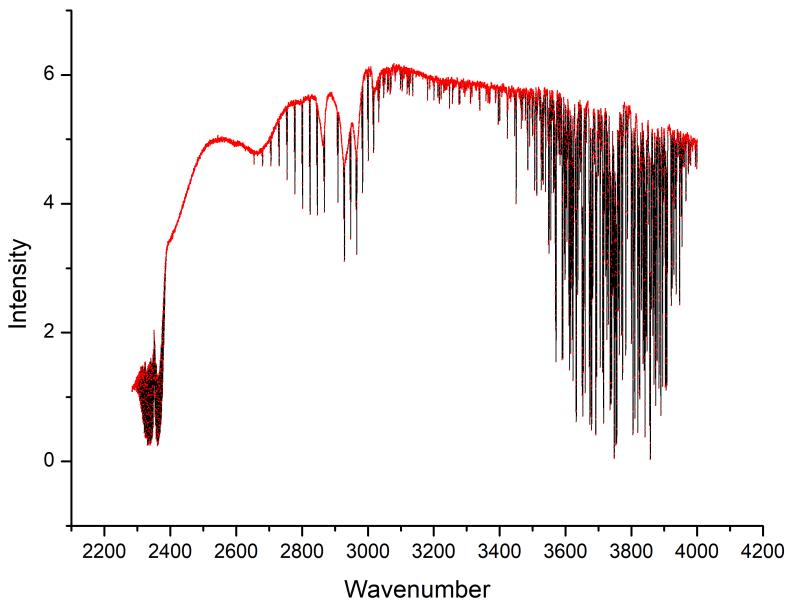


Figure 20: Original HCl spectrum.

Interpolated function was used to eliminate the background spectrum and to make it easier to determine the P – branches and R – branches.

For determining the **wavenumber of pure vibration transition** $\bar{\nu}_s$ and the **rotation constant** B equations

$$\bar{\nu}_R(0) + \bar{\nu}_P(1) = 2\bar{\nu}_s \quad \text{and} \quad \bar{\nu}_R(0) - \bar{\nu}_P(1) = 4B \quad (36)$$

were used.

Once $\bar{\nu}_s$ is known, it can be used to determine the **force constant** k according to the equation 12.

Additionally, **moment of inertia**, was resolved from definition of B 7 and this allows for the determining of **distance of the two atoms in the molecule r**.

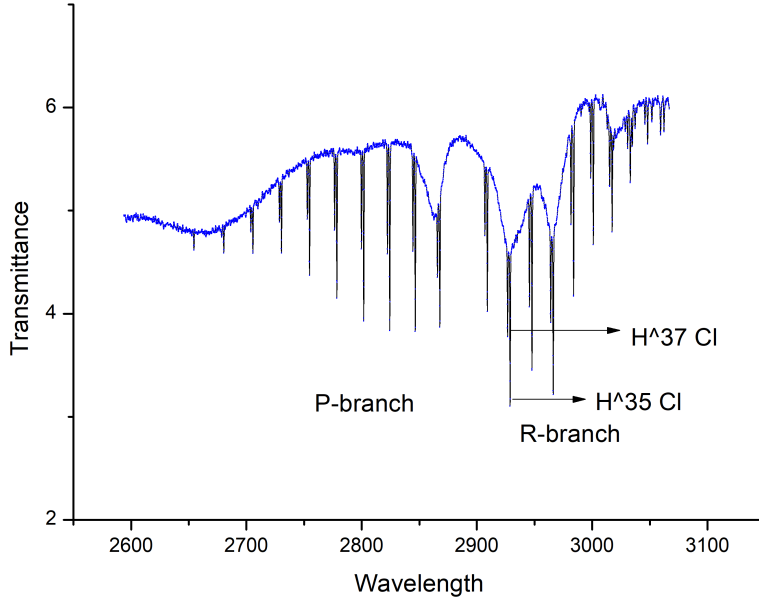


Figure 21: P-branch and R-branch of the HCl spectrum.

Furthermore, we see that our absorption line is split into two, and this effect is due to the *two isotopes of the HCl* ($H^{35}Cl$ and $H^{37}Cl$).

	$H^{35}Cl$	$H^{37}Cl$
$\bar{\nu}_R(0)$ [cm ⁻¹]	2929 (± 1.46781)	2928 (± 1.46781)
$\bar{\nu}_P(1)$ [cm ⁻¹]	2823 (± 1.46781)	2824 (± 1.46781)
$\bar{\nu}s$ [cm ⁻¹]	2876 (± 1.46781)	2876.5 (± 1.46781)
B [cm ⁻¹]	26.5	26
μ [u]	0.9797	0.9811
k [$\frac{kg}{s^2}$]	477.375	478.782
I [$kg \cdot m^2$]	$0.00105 \cdot 10^{-42}$	$0.00107 \cdot 10^{-42}$
r [m]	$8.036 \cdot 10^{-10}$	$8.106 \cdot 10^{-10}$
D [m ⁻¹]	0.0419	0.0415

Table 2: Obtained results for both isotopes.

In order to calculate the vibration rotation constant B_n and centrifugal distortion constant D , equation 25 was used.

Additionally, *running index i*, mentioned in the theory, was used to plot a graph against the wavenumbers of P- and R-branch and a cubic function fit was applied.

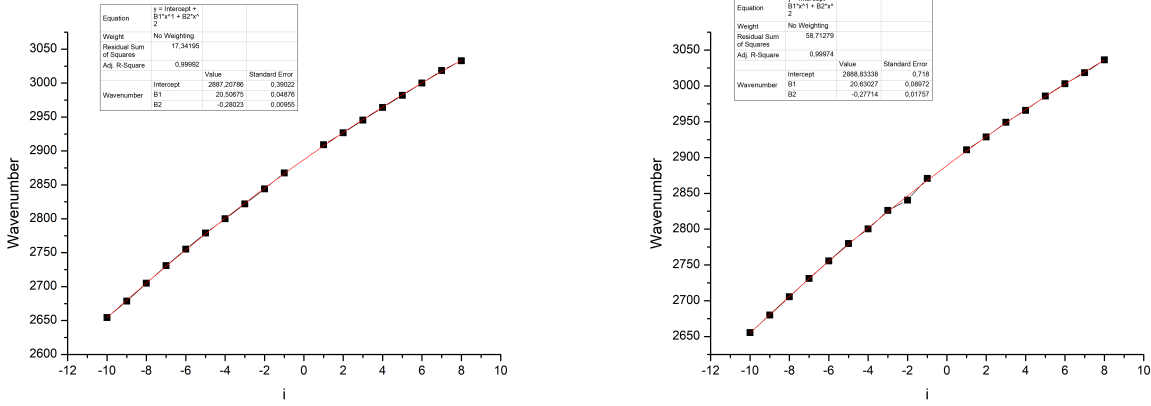


Figure 22: Running index i for both isotopes, $H^{37}Cl$ and $H^{35}Cl$ respectively, plotted and fitted with a cubic function.

Therefore, we conclude:

	$H^{35}Cl$	$H^{37}Cl$
$B_0 [cm^{-1}]$	10.13	10.14
$B_1 [cm^{-1}]$	10.42	10.43
$D [cm^{-1}]$	0.00042	0.00053

Table 3: Determining B_n and D .

5.6 Task 6

For the last task, we were asked to model the intensities of the absorption minima in the P branch using the equation 29.

Intensity peaks of P branch was determined by examining the P-branch of the HCl spectrum. Those intensities have been subsequently plotted against rotational quantum number J .

Parameter c now corresponds to the last term in the equation mentioned above and it reads:

$$c = \frac{hcB}{k_B T} \quad (37)$$

In order to determine the temperature, we rewrite the above formula and obtain $292.19K$ which is roughly the room temperature where the measurements took place.

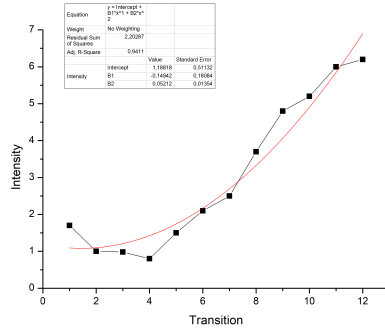


Figure 23: Transition vs intensity plot.

6 References

- [1] Rotation-Vibration Spectra of Molecules, Dr. Riede; Dr. Kranert, Fakultat fur Physik und Geowissenschaften - Advanced Physics Laboratory, Universitat Leipzig
- [2] Physical Chemistry 2nd Edition; Thomas Engel, Philip Reid; Pearson Education South Asia Pte Ltd. 2010
- [3] <https://www.shimadzu.com/an/ftir/support/tips/letter15/apodization.html>
- [4] https://en.wikipedia.org/wiki/Rotational-vibrational_spectroscopy
- [5] http://www.pci.tu-bs.de/aggericke/PC4e/Kap_III/Rot-Vib-Spektren.htm
- [6] https://en.wikipedia.org/wiki/Fast_Fourier_transform